Cureus Journal of Engineering

Open Access Original Article

Effects of Triethylamine- or Ammonium-Hydroxide-Impregnated Activated Carbon on Carbon Dioxide Capture

Received 06/17/2025
Review began 08/12/2025
Review ended 11/04/2025
Published 11/28/2025

DOI:
https://doi.org/10.7759/s44388-025-06679-y

Suravit Naksusuk [1] , Tanyarat Khongkhuntian [2] , Atichat Wongkoblap [1]

1. School of Chemical Engineering, Suranaree University of Technology, Nakhon Ratchasima, THA 2. Ratchaburi Learning Park, King Mongkut's University of Technology Thonburi, Bangkok, THA

Corresponding authors: Suravit Naksusuk, suravit@sut.ac.th, Atichat Wongkoblap, atichat@sut.ac.th

Abstract

The adsorption of carbon dioxide (CO_2) in activated carbon modified by either physical or chemical treatments was investigated in this study. The physical treatment was treated with nitrogen at room temperature and then heated to 850ºC under CO_2 gas. The chemical treatment was carried out by impregnation with either triethylamine (TEA) or ammonium hydroxide (NH_4OH). Porous properties of original and modified activated carbons were determined from N_2 adsorption isotherm at 77K. The nitrogen adsorption analysis revealed that the physical treatment increased the mesopore volume of activated carbon. Conversely, for chemically impregnated with TEA samples, the Brunauer-Emmett-Teller surface area decreased with increasing TEA concentration compared to the original activated carbon. Fixed-bed adsorption experiments demonstrated an increase of CO_2 uptake with TEA-impregnated activated carbon, while physically treated carbon exhibited similar CO_2 adsorption capacity as the original material. It was found that the maximum breakthrough time was observed for activated carbon impregnated with 1% by weight TEA solution, and then it decreased with an increase in TEA concentration (3 and 5% by weight in this study). In the study of the effect of NH_4OH on the adsorption of CO_2 on activated carbons at 298K, the isotherm obtained from the original carbon was compared with carbon impregnated with 0.05, 0.25 and 0.5% by weight of NH_4OH solutions. The adsorption in activated carbon treated with 0.05% NH_4OH solution had the maximum adsorption capacity and the adsorption capacity obtained from chemically treated activated carbons was greater than that of the original one. We also analyzed the pore volume obtained from CO_2 adsorption in carbon with and without NH_4OH, the pore volume derived from CO_2 adsorption at 298K and 1 atm was less than that obtained from N_2 adsorption isotherm at 77K. Because the saturated pressures of CO_2 at 298K and nitrogen at 77K are 64 and 1 atm, respectively, the condensation inside the pore may not be observed in the case of CO_2. The pore volume of activated carbons with NH_4OH was greater than that without NH_4OH, and this led to a greater adsorbed amount in the case of activated carbon in the presence of NH_4OH. The adsorption of CO_2 in the activated carbon with and without NH_4OH at 273K was greater than that at 298K, due to its physical adsorption behavior. In the simulation study, an early onset in the adsorption isotherm can be observed for the heterogeneous pore, especially for a smaller pore width less than 0.8 nm. The simulation result and experimental data for CO_2 adsorption at 298K agreed quite well and they could be used to describe the adsorption behavior in heterogeneous carbon. Despite this, the study identified an approach for enhancing CO_2 capture selectivity using a cost-effective preparation method that is scalable for industrial applications and real-world CO_2 capture processes.

Categories: Environmental and Sustainable Engineering, Environmental Engineering, Environmental Engineering and Sustainability
Keywords: co2 capture, fixed-bed column, monte carlo simulation, activated carbon, adsorption capacity

Introduction

Carbon dioxide (CO_2) is one of the most significant anthropogenic greenhouse gases, which is a pressing global warming concern. A large quantity of CO_2 is released from power plants and industrial sections burning fossil fuels [1,2]. An increase in the quantity of CO_2 in the atmosphere leads to a challenge for its capture and storage (CCS). Typically, there are three different processes normally used in the carbon dioxide capture: pre-combustion, post-combustion, and oxy-combustion [3,4]. For the more practical post-combustion method, four technologies-absorption, adsorption, cryogenic, and membrane-are currently employed for efficient CO_2 capture [5]. Among these, adsorption has garnered attention due to its simpler system design and lower energy requirements for regeneration compared to chemical absorption [6-9]. Although, CO_2 absorption by liquid amine has been widely used due to its high removal

How to cite this article
Naksusuk S, Khongkhuntian T, Wongkoblap A (November 28, 2025) Effects of Triethylamine- or Ammonium-Hydroxide-Impregnated Activated Carbon on Carbon Dioxide Capture. Cureus J Eng 2 : es44388-025-06679-y. DOI https://doi.org/10.7759/s44388-025-06679-y

efficiency [10], this process has many shortcomings, such as high corrosion, high power consumption for amine recovery, and high cost.

The adsorption process is one of the interesting technologies for several reasons, i.e., the low cost of materials used as adsorbents, low energy for adsorbent regeneration, and extremely high efficiency [11]. Porous materials known as adsorbents play a crucial role in the adsorption process. Common adsorbents include metal-organic frameworks (MOFs), zeolites, activated carbon, and clays. Activated carbon is a porous carbon material that is widely used as an adsorbent and stands out for its high internal surface area, large amounts of micropores, high adsorption capacity, low cost, and ease of production from biomass. Generally, activated carbon can be prepared by a two-step physical activation and chemical activation methods. Many researchers have reported the preparation of activated carbon from a variety of agricultural wastes such as coconut shells, walnut shells, eucalyptus, argan fruit shells, longan seeds, corn stalks, and other biomass-derived materials [12-15]. Activated carbon, which consists mostly of micropores, is typically used for gas adsorption, including carbon dioxide. To increase CO_2 capture efficiency, the researcher has developed different preparation techniques to synthesize the activated carbon with superior adsorption capacity [10,13]. However, its inherent lack of selectivity toward CO_2 requires surface modification to enhance capture efficiency. Many modification techniques are costly, complex, and yield relatively low productivity [16-21].

Since CO_2 is an acid gas, using an adsorbent with more active basic sites will help improve the capacity and selectivity of CO_2 adsorption. The simplest technique used for introducing basic sites on the surface of an adsorbent is by impregnating the adsorbent with basic alkali solutions. To improve CO_2 selectivity, many engineers and scientists have been investigated the role and efficiency of various impregnation solutions, such as sodium hydroxide (NaOH), potassium hydroxide (KOH), metal oxide and amine solutions, on CO_2 adsorption capacity [21,22]. In the case of amine-based solutions, such as monoethanolamine (MEA), diethanolamine (DEA), and triethanolamine (TEA) have demonstrated effectiveness in CO_2 capture. While MEA and DEA have been extensively studied due to their strong affinity toward acidic gases, TEA has received relatively little attention. This presents an opportunity for further investigation, especially given TEA's advantages such as lower volatility and reduced corrosiveness. Therefore, this study explores the use of TEA for modifying activated carbon to enhance CO_2 capture performance. In the meantime, ammonium hydroxide (NH_4OH) as an alkaline solution, which is composed of ammonium and hydroxyl groups, has been paid less attention to carbon dioxide capture. Therefore, the effects of NH_4OH on CO_2 adsorption with different impregnated alkaline concentration will be revealed by using a Grand Canonical Monte Carlo (GCMC) simulation.

Therefore, the main purpose of this investigation is to improve the efficiency of commercial activated carbon for CO_2 capture. The effectiveness of physical and chemical modification techniques for activated carbon to enhance CO_2 adsorption is performed in either a fixed-bed adsorber or an adsorption tube. The surface modification by physical treatment involves the gasification of activated carbon with air and CO_2 while the chemical modification is conducted using TEA solutions of varying concentrations or the impregnation of activated carbon in NH_4OH solutions. Both treatments are selected for their potential scalability in industrial applications. Furthermore, this exploration proposes a finite-length slit pore model in the absence or presence of ammonium hydroxide with different loadings to investigate the mechanism of CO_2 adsorption in different pore widths. The measurement of N_2 adsorption isotherms of prepared activated carbon was performed at -196°C (77K) for the porous structure investigation. The adsorption of CO_2 in activated carbon with and without TEA was measured at 35°C (308K) in the fixed-bed adsorber to evaluate the impact of physical and chemical treatments on CO_2 uptake and adsorbate diffusivity, assessed through breakthrough curve analysis. The adsorption of CO_2 in activated carbon containing NH_4OH was performed in a surface area analyzer (ASAP2020) at 25°C (298K) to assess how alkaline loading affected the adsorption capacity. The effects of temperature or ammonium hydroxide on carbon dioxide adsorption in the slit pore model are also studied.

This paper presents the methodology for activated carbon modification, experimental, and GCMC simulation procedures. It also provides the porous properties of activated carbon obtained from the N_2 adsorption isotherm and the effects of TEA loading on the adsorption of CO_2 in a fixed-bed adsorber. The effects of NH_4OH on the adsorption behavior of CO_2 obtained from the experiment and simulation are also discussed. A comparison of experimental data and simulation results is provided. Finally, the conclusion is summarized. The outcome of this study provides an alternative method for improving CO_2 capture efficiency in activated carbon and understanding the adsorption behavior in porous materials.

Materials And Methods

Materials

The activated carbon used in this study is a commercial activated carbon produced from coconut-shell by steam activation. It was supplied by Right Reactivation Public Company Limited in Rayong, Thailand, and an average particle size was reported as 1.29 mm (14 × 16 mesh screen size). CO_2 and N_2 gases, with a purity of 99.9%, were purchased from Linde (Thailand). The TEA solution (99.9%) and ammonium hydroxide (35%) was obtained from Chemipan Corporation Co., Ltd., Thailand.

Physical and chemical treatment processes

For physical treatment, activated carbon was treated with N_2 gas at room temperature and then heated to 850°C. Followed by a switch to CO_2 and held at 850°C for 2 hours. This sample was called AC-P. For chemical treatment, an impregnation process with a TEA solution was used. TEA-impregnated activated carbon was prepared by mixing 50 g of activated carbon in 180 cm^3 of TEA solution of the desired concentration (1-5 wt% TEA). The mixture was then shaken in a water bath at room temperature using a shaking speed of 180 rpm for 90 minutes to reach equilibrium. Next, the sample was dried in an oven at 110°C for 48 hours. Each impregnated carbon was given a sample name that consisted of the activated carbon (AC), followed by the name of the impregnating substance (TEA), and the weight percentage of the TEA solution used for the impregnation.

The chemical treatment for NH_4OH impregnated activated carbon was prepared by soaking 50 g of the activated carbon in 400 cm^3 of NH_4OH solution of the desired concentration (in weight% NH_4OH) for 8 hours at 70°C and dried in an electric oven at 105℃ for 12 hours. And then all samples were placed in the Desiccator, until they were cooled at room temperature. The concentration of NH_4OH solution varied in the range from 0 to 0.5% by weight, corresponding to the NH_4OH loading of 0-398 mg NH_4OH/g carbon. The concentration of NH_4OH solutions of 0.05, 0.25 and 0.5% was related to the amount of impregnated NH_4OH of 39, 199, and 398 mg NH_4OH/g carbon, respectively.

With the impregnation method, most of amine or alkaline will diffuse into the inner pores of activated carbon at low concentration. When the concentration of solutions increases, the molecules of either TEA or NH_4OH will distribute not only inside the pores but also at the external surfaces of carbon as shown in the literature [23].

Experimental adsorption isotherm and pore characterization

The porous properties of the original, physically treated, and TEA-impregnated activated carbon were determined from the nitrogen adsorption isotherms measured at -196°C (77K) using the surface area analyzer (ASAP2020, Micromeritics, USA). The resulting N_2 isotherms were used to compute the total surface area of each carbon sample using the Brunauer-Emmett-Teller (BET) equation [24]. The t-plot approach was used to calculate the micropore volume [25]. The total pore volume was calculated using the quantity of gas adsorbed at the relative gas pressure (P/P^0) of 0.98, which was then translated to the volume of N_2 in the liquid form. The average pore diameter was determined using the equation 4V/A, where V and A stand for the total pore volume and BET surface area, respectively, based on the assumption that the pores were cylindrical in shape. The porous carbon model can be assumed to consist of pores of different widths that can be either infinite slit pores or infinite cylindrical pores. It was reported in the literature [26], that if the mesopore structure consists of a set of open-ended, non-intersecting cylinders, the mean pore radius, r, is given by,

$$r = 2V/A$$

based on the assumption that the specific surface area is confined to the cylindrical pore walls, in which, $2r = D = 4V/A$. Therefore, in the evaluation of average pore size of activated carbon, the cylindrical pore model is used, but in simulation study, activated carbon model is assumed to be slit pore model.

Fourier Transform Infrared Spectroscopy (FTIR, Tensor 27) was used to characterize functional groups on the surface of activated carbon. Scanning Electron Microscopy (SEM, JSM-6010LV) was used to characterize surface morphology of samples.

The adsorption isotherm for CO_2 in activated carbon in the presence and absence of NH_4OH at 25°C (298K) was measured by the surface area analyzer (ASAP2020, Micromeritics, USA). The obtained isotherm was used to determine the total pore volume and average pore size, and the surface morphology of carbon samples was determined by SEM. The measured isotherm was optimized with the nonlocal density functional theory isotherms of CO_2 at sub-atmospheric pressures, and t-plot method was used to determine the pore volume. The characterization of fine microporosity of activated carbon, where CO_2 was used as a probing molecule for the narrowest micropores at experimentally measurable pressures, and

good agreement with adsorption capacity can be observed as described in the literature [27].

Nitrogen at 77K and pressures up to 1 atm were used to characterize the porous properties of both TEA and NH_4OH activated carbon series. In the case of TEA carbon series, we would like to study the kinetics adsorption of CO_2 using packed bed column, then the porous properties obtained by CO_2 adsorption isotherms were not determined. But in the case of NH_4OH carbon series, we intended to study the equilibrium adsorption of CO_2 inside the pores, and some porous properties were determined, because the CO_2 isotherms measured up to 1 atm were not sensitive to pores wider than 1 nm [27]. We also would like to use simulation study to explain the adsorption behavior of CO_2 in activated carbon in the presence and absence of NH_4OH.

Fixed-bed adsorption

The research involved conducting CO_2 adsorption in original, physically treated, and TEA-impregnated (as a chemical treatment) activated carbons in the fixed-bed adsorber. The column used in this study was a transparent acrylic column with a 1 cm diameter and 60 cm height. The adsorption temperature was maintained at 35°C (308K) by circulating water from a temperature-controlled water bath through the column jacket. The experimental procedure involved purging the column with nitrogen gas for 15 minutes at a flow rate of 100 cm^3/min, followed by filling the column with activated carbon to the desired height. Then, a gas mixture of nitrogen and CO_2 was allowed to flow through the column, and the CO_2 concentration was adjusted to 13 vol% (the average CO_2 concentration in flue gas from solid fuel combustion) using a portable gas analyzer (BIOGAS 5000, Geotech, UK). The gas flow rates were adjusted to achieve this concentration level. The timing process started once the feed gas mixture was added to the adsorption column. The exit concentration of CO_2 was measured as a function of time until the concentration began to approach the input concentration. The gas flow rates and the feed gas composition were kept constant throughout the experiment. The experimental conditions for the adsorption investigation were summarized in Table *1*.

Conditions	Values
TEA solution (wt%)	0-5
%CO_2 in the feed gas (vol%)	13
Gas superficial velocity (cm/s)	3.03
Temperature (^OC)	35
Amount of carbon (g)	10
Bed height (cm)	28.2

TABLE 1: Experimental conditions for CO2 adsorption in the fixed-bed column

TEA, triethanolamine

The Monte Carlo simulation

In this investigation, the adsorption isotherms of CO_2 in finite-length slit pore model at 273 and 298K were obtained by using the GCMC simulation. The Metropolis algorithm in the Monte Carlo (MC) simulation was applied to evaluate the adsorption equilibrium by specifying the pore volume (V), the system's temperature (T), and the chemical potential (μ) [28]. The activated carbon was modeled as slit pore with two parallel walls, each wall consisted of three graphene layers and finite in length having a linear dimension of 6 nm in X (Lx) and Y (Ly) axes [29,30]. The distance between these two walls in Z axis was defined as pore width (H) and was specified in the range of 0.65 to 5.0 nm to form the kernel of adsorption isotherms. Each graphene layer of the pore wall had an interlayer spacing (Δ) of 0.335 nm and was composed of carbon atoms in a hexagonal arrangement with the bond length between carbon atoms of 0.142 nm. The collision diameter of carbon atom (σ_{ss}) was 0.34 nm and the energy well depth (ε_{ss}/k) was 28K.

The absence and presence of NH_4OH molecules on the carbon slit pore model were shown in Figure *1*. In

this investigation, NH_4OH molecules were placed on the surface of slit pore near the pore mouth with 0.5% loading, for which the number of NH_4OH molecules on two carbon surfaces determined by GCMC simulation was 36. The molecular parameters for NH_4OH were based on the similar behavior of NaOH as follows: $\sigma_{O\text{-}O}$ = 0.3804 nm, $\varepsilon_{O\text{-}O/kB}$ = 1962K, q_O = − 1.056e, q_H = 0.298e, and then q_{NH4} = 0.758e. The bond length between the hydrogen and oxygen atoms was 0.097 nm, and that between NH_4 and oxygen atoms was 0.2335 nm. The bond angle of N-H-O was about 153.6° and the bond angle of H-N-H was about 107.29°. The center of the oxygen of the NH_4OH group was far from the pore wall, about 0.37 nm and perpendicular to the wall [31,32].

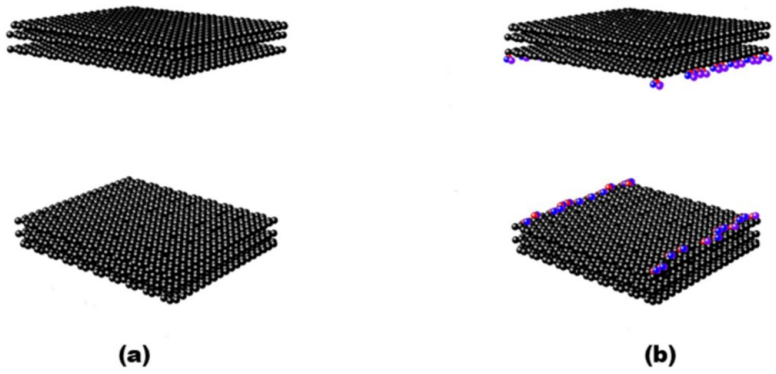

FIGURE 1: Activated carbon models (a) without NH4OH and (b) with NH4OH, where black sphere symbols are carbon atoms, purple sphere symbols are NH4 molecules, red sphere symbols are oxygen atoms, and blue sphere symbols are hydrogen atoms

One GCMC cycle consisted of one thousand moves with equal probability of displacement moves, insertion of the new particle and attempt to delete the old particle. CO_2 was modeled as three centers Lennard Jones (LJ) model and had molecular parameters as shown in Table *2* [33]. In each move, CO_2 was also randomly rotated around the x, y, or z axes with equal probability. In each specified pressure, 40,000 GCMC cycles were required for the system to attain adsorption equilibrium and additional 40,000 GCMC cycles were needed to establish ensemble averages. The equation of state proposed by Johnson et al. [34] was used to predict the bulk pressure associated with a given chemical potential. The adsorbed amount at each point in the simulation result was estimated as pore density (ρ) from equation (1).

$$\rho = \frac{N_{\text{inside}}}{V_{\text{pore}}} \quad (1)$$

where N_{inside} was number of particles inside the pore, and the pore volume (V_{pore}) was defined as Lx × Ly × H

Parameter	Value	Parameter	Value
σ^{c-c}	0. 2757 nm	ε^{c-c}/k	28.129K
σ^{o-o}	0.3033 nm	ε^{o-o}/k	80.507K
q^{c}	0.6512e	q^{o}	-0.3256e
λ^{c-o}	0.1149 nm		

TABLE 2: Molecular parameters for carbon dioxide

where σ is the collision diameter, ε is the energy well depth, q is the electrostatic charge, and λ is the separation distance between carbon atom and oxygen atom of CO2 in the simulation model which is the bond length.

Results

Effects of triethylamine (TEA) on adsorption isotherm

Adsorption of N_2 in Original and Modified Surface of Activated Carbons and Porous Properties

The typical nitrogen adsorption-desorption isotherms of the studied activated carbons are depicted in Figure *2*. The isotherms exhibit a Type I isotherm according to IUPAC classification, indicating a sharp rise in adsorption at low pressures followed by a plateau at high pressures [35]. This suggests a predominantly microporous structure, which is further confirmed by Table *3*. The micropore area of all samples ranges from approximately 70% to 88%. TEA-impregnated activated carbon shows lower N_2 adsorption than AC-P and AC. This is likely due to the TEA coating on the activated carbon surface, which may interfere with nitrogen molecule adsorption onto the graphene layer. Similar behavior of nitrogen adsorption can be observed in the case of AC-TEA1 and AC-TEA3 as shown in the insertion of Figure *1* and the adsorption decreased with an increase of TEA to 5% (AC-TEA5). This may be due to the pore blocking effect of TEA loading, hindering N_2 diffusion to the inner adsorption sites. Increasing TEA loading leads to a decrease in both surface area and pore volume. The surface area of TEA-impregnated activated carbon is reduced by approximately 43.5% with increasing TEA loading.

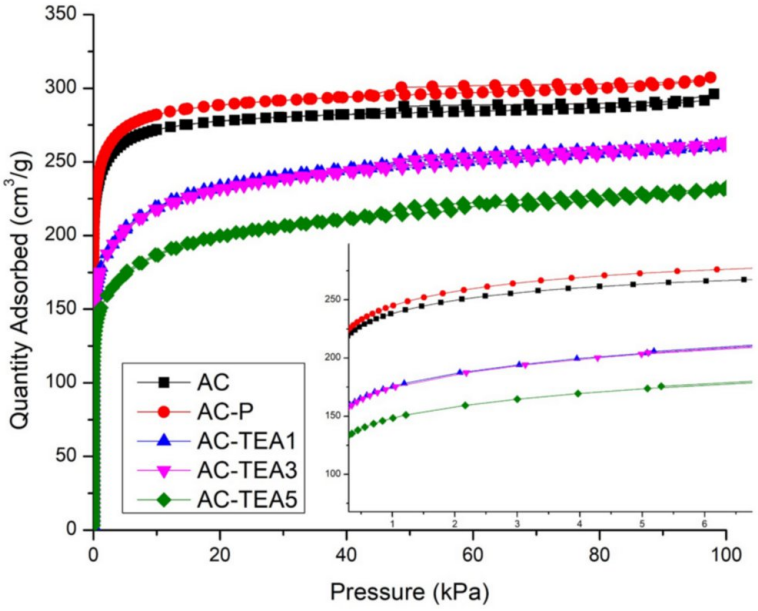

FIGURE 2: N2 adsorption and desorption isotherm of original activated carbon (AC), physical treatment activated carbon (AC-P), and TEA-impregnated activated carbons (AC-TEA)

Samples	BET surface area (m^2/g)	[1]Micropore area (m^2/g)	[1]Micropore volume (cm^3/g)	[2]Total pore volume (cm^3/g)
AC	1,081	960	0.3765	0.4117
AC-P	1,118	986	0.3888	0.4275
AC-TEA1	756	502	0.2482	0.3238
AC-TEA3	749	504	0.2497	0.3402
AC-TEA5	649	416	0.2053	0.2946

TABLE 3: Porous properties of original, physically treated, and TEA-impregnated activated carbons

[1] t-plot
[2] DFT

TEA, triethanolamine

Functional Groups and Surface Morphology Determination for TEA-Impregnated Activated Carbons

FTIR spectra of AC, AC-P, and AC-TEA1 were collected to characterize their surface functional groups as shown in Figure *3*. These samples were compared to the original activated carbon, both physically and chemically treated. AC exhibits a peak at 3700-3584 cm^{-1}, attributed to O-H stretching, indicating the presence of alcohol groups. Additionally, peaks at 1440-1395 cm^{-1} and 1390-1310 cm^{-1} suggest the presence of carboxylic acid and phenol groups, respectively. C=C bending is observed at 995-665 cm^{-1}. AC-P shows CO_2 groups at 2349 cm^{-1}, likely due to the CO_2 gasification treatment, and a strong peak at 1550-1500 cm^{-1} indicative of nitro compounds. AC-TEA1 exhibits a C-N peak at 1250-1020 cm^{-1}, suggesting the presence of amine groups introduced by the TEA solution impregnation [35]. These findings confirm that both physical and chemical treatments can increase active sites as functional groups on carbon surface

which may enhance the adsorption capacity and selectivity for CO_2 adsorption. Further investigation of CO_2 capture will be discussed in the next section.

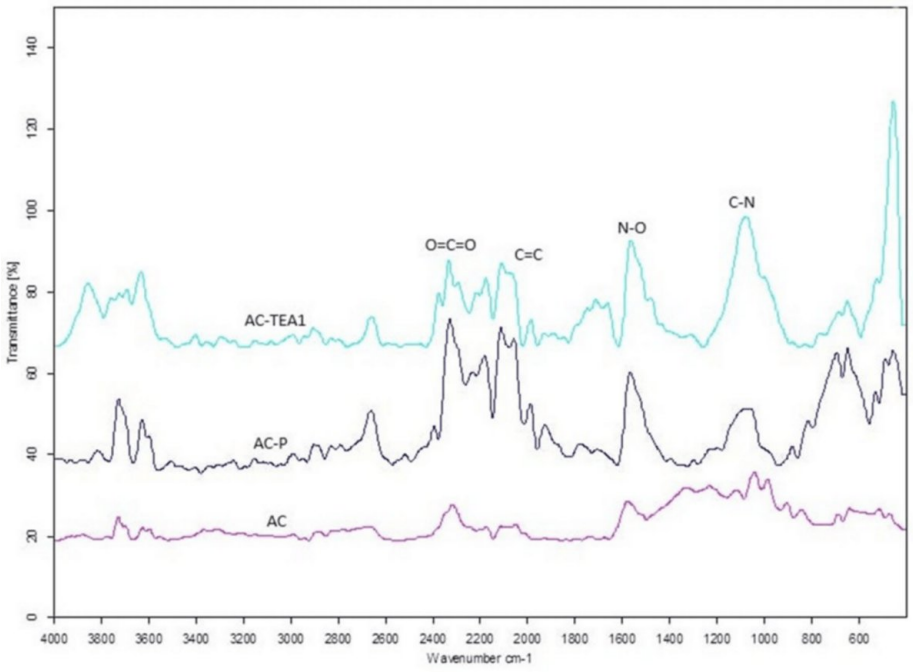

FIGURE 3: FTIR spectrum of original activated carbon, physical treatment activated carbon, and TEA-impregnated activated carbon

TEA, triethanolamine; FTIR, Fourier Transform Infrared

Surface morphology studies of original (AC), physical treatment (AC-P), 1% TEA solution impregnated (AC-TEA1), 3% TEA solution impregnated (AC-TEA3), and 5% solution impregnated (AC-TEA5) activated carbons are illustrated in Figure *4* (a), (b), (c), (d) and (e), respectively. AC shows a porous structure, while AC-P exhibits a higher number of pores within its structure. The amount of micropores in the AC-P is greater than that observed in the original carbon (AC) because the pore collapse of mesopores occurs at high temperature. While the TEA-impregnated activated carbon appears to have a glaze-like coating on its surface, which may close the pore mouth at higher TEA concentrations (5%). As one can see, the pore size of activated carbons treated with TEA becomes larger than the original and physical treatment carbons. The growth of mesopores is developed because of the micropores widening during the chemical treatment and the pore size becomes larger as an increase of TEA concentration. This leads to the lower BET surface area, micropore area, micropore volume, and total pore volume as shown in Table *3*.

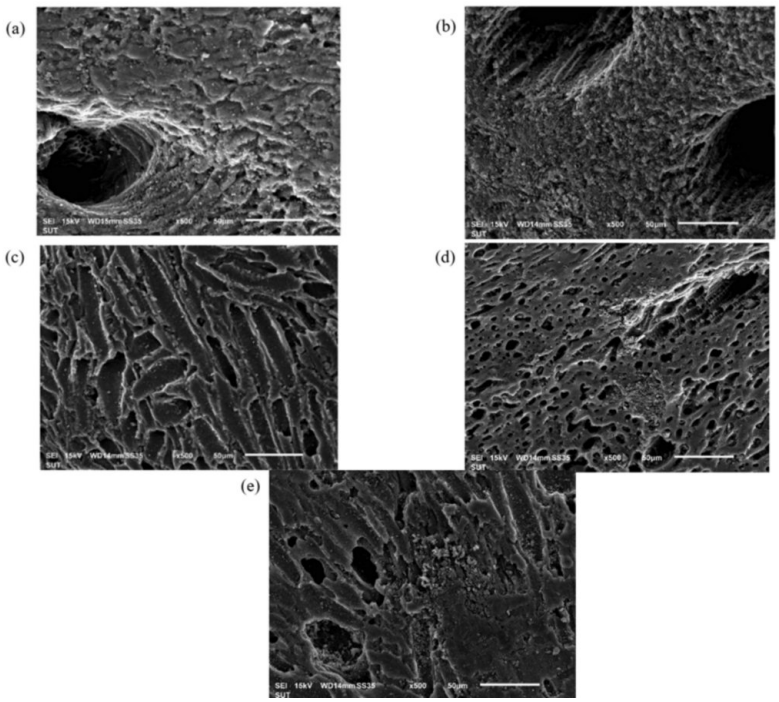

FIGURE 4: Scanning Electrons Microscope of original activated carbon, physical treatment activated carbon, and TEA-impregnated activated carbon. (a) AC, (b) AC-P, (c) AC-TEA1, (d) AC-TEA3, and (e) AC-TEA5

TEA, triethanolamine

CO_2 Adsorption in ACs Using Fixed-Bed Adsorption

Adsorption behavior of CO_2 in the fixed-bed adsorber for the original AC, AC-P, and activated carbons impregnated with 1-5% TEA loadings (AC-TEA) were carefully investigated, and the typical S-shaped breakthrough curves were observed as shown in Figure *5*. The breakthrough curve showed the correlation between adsorption time in the X-axis and the value of outlet and inlet concentration ratio (C/C_0) in the Y-axis. The "breakthrough time (t_B)" itself refers to the point at which the downstream CO_2 concentration reaches 5% of its initial value ($C/C_0 = 0.05$), which is a crucial threshold for industrial applications. At breakthrough time, the operation of the adsorber column will be stopped and it needed to regenerate the adsorbent. One of the main conclusions was that the observed breakthrough times and the TEA content were directly correlated. The breakthrough curve analysis reveals that the AC-TEA1 had the maximum breakthrough time, and it decreased with an increase of TEA (AC-TEA3 > AC-TEA5 time). The breakthrough time obtained for original activated carbon (AC) showed the lowest time and less than that for modified activated carbon with physical treatment (AC-P). The breakthrough times for each type of carbons were presented in Table *5*. The mechanism of adsorption in a fixed-bed column was the diffusion of gas molecules through the column bed and the pores of the activated carbon, and surface functional groups had a significant influence on the placement of the curve. As one can see in Table *4* that the adsorption capacity at the breakthrough time of TEA-impregnated activated carbons exhibited the greater adsorbed amount than the original one (AC). TEA impregnation behaved as functional groups that enhanced CO_2 adsorption compared to unimpregnated carbons. For fixed-bed columns, the impregnation with 1% amine solution had relatively constant diffusivity; however, the concentration of TEA loading increased led to the diffusivity decreasing trend. Similar behavior can also be observed in the literature [23]. This reduction is commonly attributed to the physical obstruction of pores by the impregnating agent of TEA.

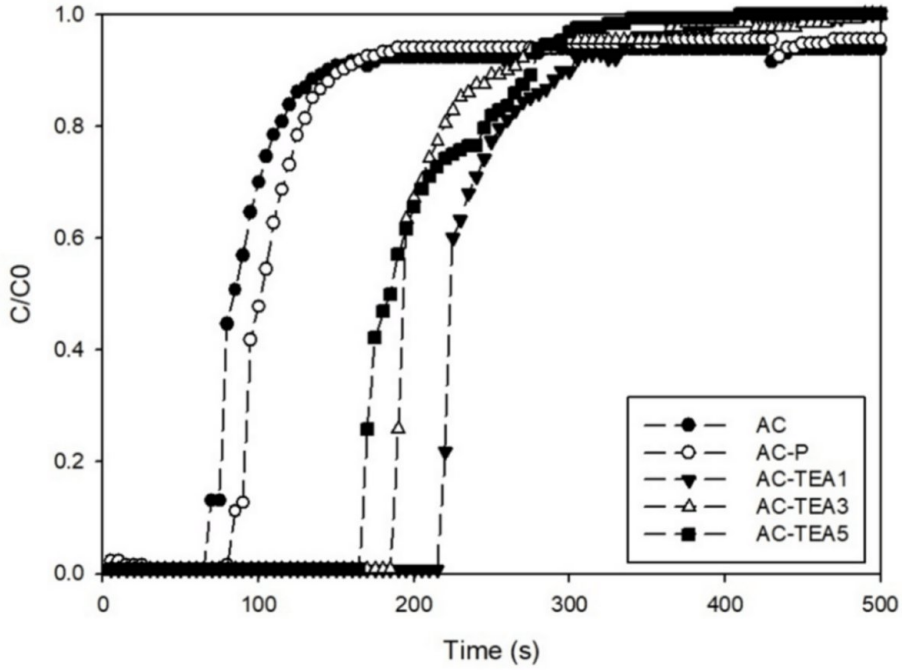

FIGURE 5: Breakthrough curve of CO2 adsorption in a fixed-bed column

Samples	Breakthrough time (t_B, sec)	CO_2 adsorption capacity at t_B (mg CO_2/g carbon)
AC	70	9.92
AC-P	80	11.6
AC-TEA1	209	29.8
AC-TEA3	180	25.7
AC-TEA5	160	22.9

TABLE 4: CO2 adsorption capacity of all samples in fixed-bed absorber

To quantify the adsorption efficiency, the adsorption capacity at the breakthrough point (q_B) was determined via equation (2), a calculation that integrates the outlet (C) and inlet (C_0) CO_2 concentrations, the feed gas's volumetric flow rate (Q), and the mass of the activated carbon (W)

$$q_B = \frac{C_0 Q}{W} \int_0^{t_B} \frac{1 - C}{C_0} dt \quad (2)$$

where C and C_0 are the outlet and inlet concentrations of CO_2, respectively, Q is the volume flowrate of the feed gas, and W is the weight of activated carbon.

Adsorption of CO_2 in activated carbons impregnation with NH_4OH

Experimental Adsorption Isotherm and Pore Structure

The adsorption of CO_2 at 25°C (298K) for activated carbons with and without NH_4OH impregnation is shown in Figure 6. The adsorbed amount obtained for the 0.05% weight of NH_4OH solution is the greatest, at 58.8050 cm^3/g STP, which is close to that obtained for 0.5% NH_4OH solution, at 58.7648 cm^3/g STP. The original carbon without NH_4OH has an adsorption capacity of 54.7059 cm^3/g STP, which is the

lowest adsorbed amount in this study. This may be because the initial adsorption occurred at the alkaline group, where the interaction between CO_2 molecule and NH_4OH is greater than that between fluid and solid. When the alkaline concentration increases too much, it may cause a pore-blocking effect and lead to the lower adsorption of CO_2. This is due to the difficulty of CO_2 molecules diffusing through the pore mouth. Therefore, NH_4OH can enhance the adsorption of CO_2 at low pressures, and this will be further investigated in the molecular simulation section.

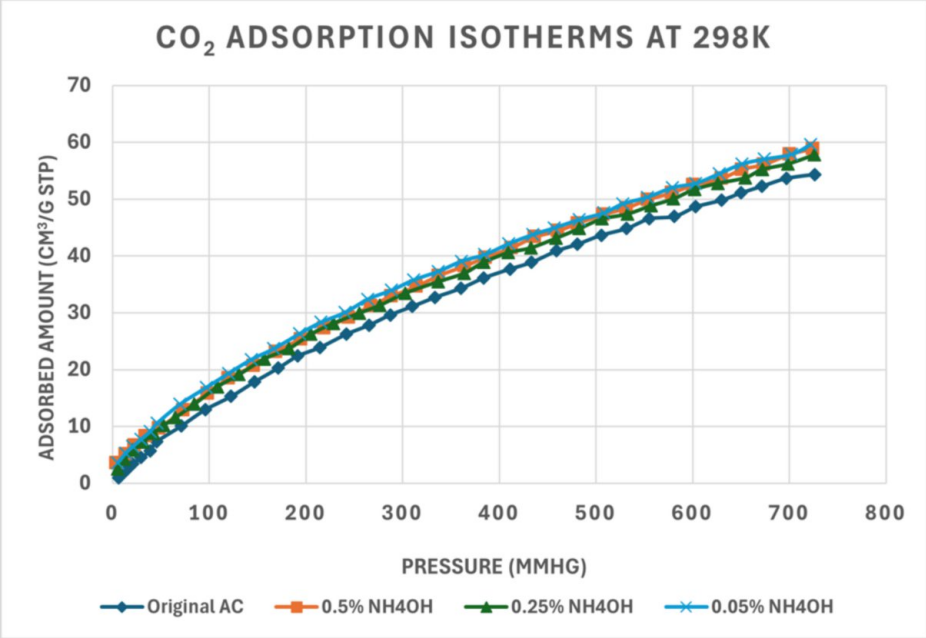

FIGURE 6: Experimental isotherms for CO2 adsorption in activated carbons with various NH4OH concentrations at 298K

The adsorption of CO_2 can be used to study the porous properties of adsorbent, and the porous properties of carbon in the presence and absence of NH_4OH is presented in Table *5*. The total pore volume of activated carbon impregnated with NH_4OH is greater than that of the original carbon, about 12% (increases from 0.0800 to 0.0910 cm^3/g). However, the average pore size for carbon with NH_4OH impregnation is greater than that without chemical treatment, which is similar to that observed in the case of TEA treatment. The surface morphology of activated carbons revealed a significant change in the case of NH_4OH impregnation, the micropore volume increased due to some mesopores collapsing by chemical treatment and led to the total pore volume increasing. Figure *6* shows the particles of NH_4OH on the carbon surface allocated at the pore mouths, which may lead to the average pore size becoming greater. It is noted that the porous properties obtained from CO_2 adsorption isotherms at 298K are less than those from N_2 adsorption isotherm at 77K, because the adsorption capacity of CO_2 does not reach the saturated condition as N_2. The saturated pressure of CO_2 at 298K is 64 atm while that of N_2 at 77K is 1 atm. In this study, the adsorption in activated carbon for CO_2 at 298K and that for N_2 at 77K were carried out at 1 atm. Therefore, the condensation inside the pore cannot be observed and it does not reach the saturated condition in the case of CO_2 at 298K. Thus, all pores are not filled with the condensed phase of CO_2. But N_2 can condense inside the pore at 77K due to approaching the saturated pressure. The larger average pore size in the case of carbon with the presence of NH_4OH may be due to the widening of micropores with an increase of alkaline concentration, as observed in Figure *7* (a)-(d) of SEM images.

CO_2 adsorption		
Activated carbon	Pore volume (cm^3/g)	Pore size average (nm)
AC original	0.0800	1.00040
AC + NH_4OH 0.05%	0.0910	1.23510
AC + NH_4OH 0.25%	0.0890	1.18400
AC + NH_4OH 0.5%	0.0909	1.20830

TABLE 5: The porous properties of activated carbon obtained from CO2 adsorption isotherm

Figure 7 (a), (b), (c) and (d) present the SEM images of original carbon and carbon with 0.05, 0.25, and 0.5% of NH_4OH solutions impregnation, respectively. It is found that an increase of NH_4OH loading can increase the pore volume. A glaze-like coating on carbon surfaces was similar to that observed in the case of TEA series when the NH_4OH loading increased. Although the average pore size become larger than that of the original carbon, the total pore volume is greater than the original carbon volume too. The greater pore volume can enhance the greater adsorbed amount of CO_2, and therefore the impregnation of activated carbon in NH_4OH solution can be used to modify the carbon surfaces for CO_2 capture and storage.

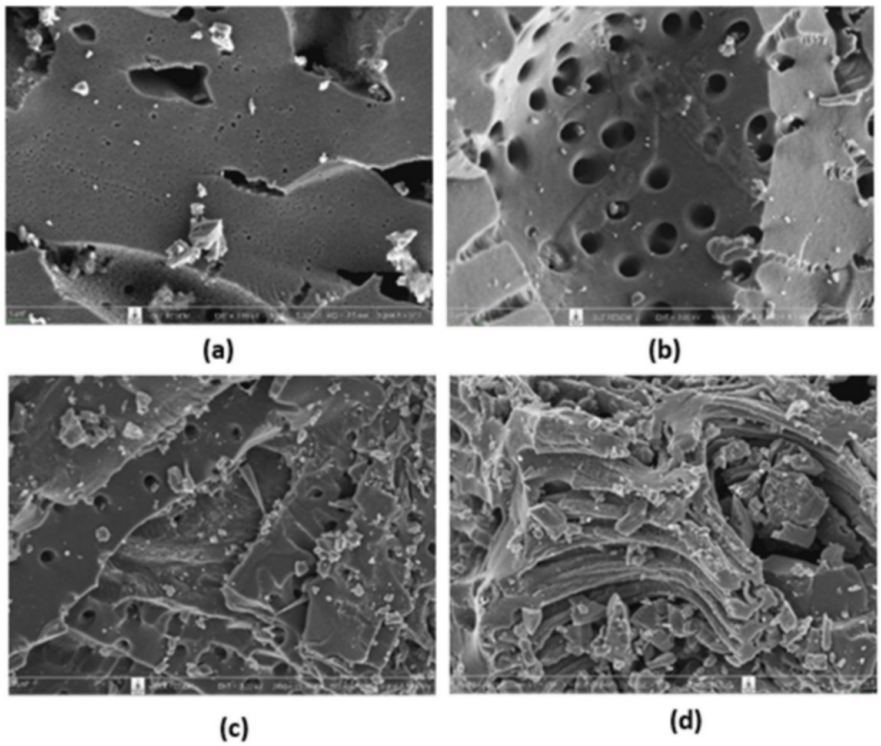

FIGURE 7: Scanning Electron Microscope images of original activated carbon: (a) original, (b) 0.05% NH4OH, (c) 0.25% NH4OH, and (d) 0.5% NH4OH

Molecular Simulation Results

Figures 8 and 9 illustrate the CO_2 adsorption isotherms versus pressure by using the GCMC simulation method at 273 and 298K, respectively. Each figure showed the set of isotherms obtained for single carbon

slit pore in the presence of NH_4OH for pores having widths of 0.65 to 5.0 nm. The continuous isotherm of a monolayer was attained for a width of less than 0.8 nm and the maximum capacity can be observed for pore width of 0.65 nm because CO_2 can fit tightly inside the pore as a single layer. As pore sizes increased, the adsorption capacity decreased because of the packing effect which caused the different maximum densities in each pore width. In the case of pore widths between 0.9 and 1.2 nm, a gradual increase of adsorption isotherm can be observed; CO_2 molecules can form a monolayer along each pore wall. For slit pores larger than 1.2 nm, the slight change of adsorption isotherm can be observed because, after the formation of monolayer, the additional layers adjacent to the monolayer can be formed until it reaches saturation. For the larger pore widths of 2.0 to 5.0 nm, the layering followed by pore-filling mechanism was visible. The adsorption isotherms gradually increased because of the layering phenomena, and at high pressures, the adsorption isotherm showed a small jump due to pore-filling behavior. When the adsorption of the fluid occurs in the larger mesopores, capillary condensation can be observed.

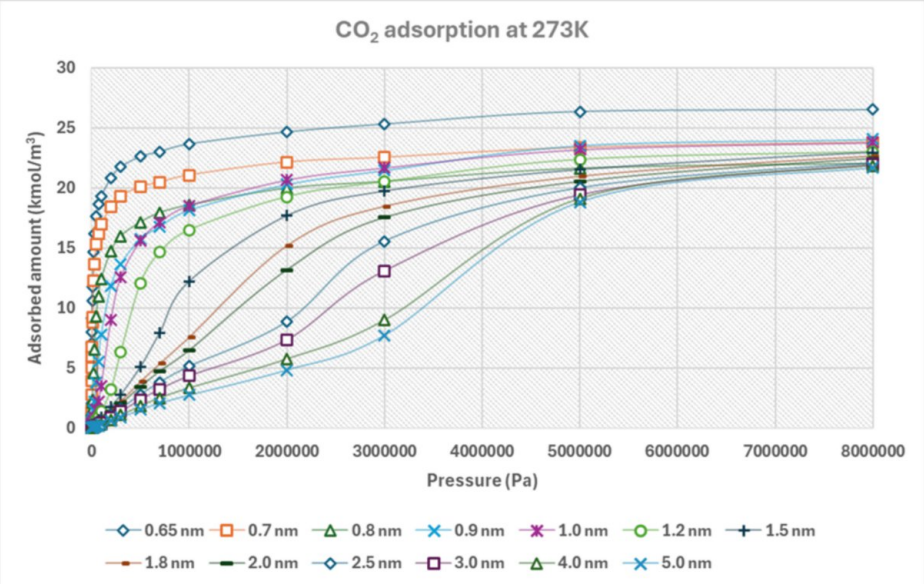

FIGURE 8: Simulation results for CO2 adsorption in activated carbons with NH4OH loading at 273K

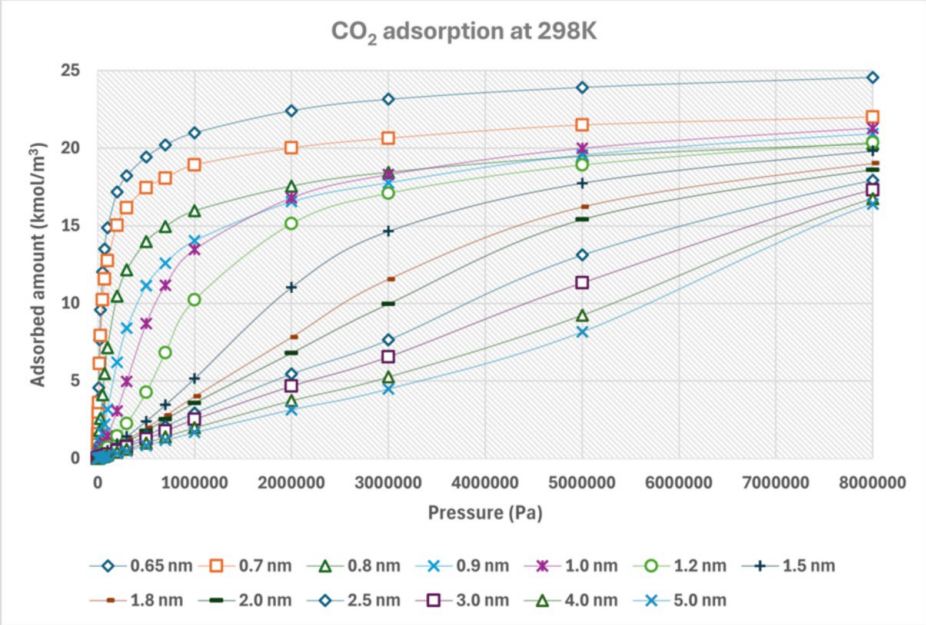

FIGURE 9: Simulation results for CO2 adsorption in activated carbons with NH4OH loading at 298K

The CO_2 adsorption isotherms for each pore width at 273K showed in Figure *8* were compared with those at 298K presented in Figure *9* to investigate the effect of temperature on adsorption isotherms. Based on our observation, the adsorption isotherm decreases as the temperature rises, as is the typical behavior in the case with physical adsorption. The reason for this is that adsorption is an exothermic process, meaning that the molecules that are adsorbed gain more energy to evaporate. The discussion for the effect of NH_4OH on adsorption isotherm and the comparison between homogeneous and heterogeneous pores will be discussed in the next section.

Discussion

Effects of NH_4OH on adsorption isotherm using the GCMC

The adsorption isotherm of CO_2 in pores having widths of 0.65, 1.0, 1.5 and 2.0 nm were also shown in Figures *10* (a)-(d), respectively, to study the adsorption behavior of the fluid in different pore widths in the presence and absence of NH_4OH at 273K. Effects of NH_4OH on adsorption isotherm for CO_2 in different pore widths at 273K can be summarized as follows:

(a) An early onset in adsorption isotherm can be observed in pore with NH_4OH, especially in the case of pore having widths less than 1.5 nm. This is similar to that observed in the experiment.

(b) The initial adsorption occurred at NH_4OH due to the stronger interaction between CO_2 and NH_4OH, and it occurred at lower pressures when the pore was smaller.

(c) At high pressures, after pore filling occurred, the adsorption isotherm obtained for CO_2 in heterogeneous pore became less than that in the homogeneous pore. This may be due to the less accessible volume than the pore volume specified in the simulation box. Then, the number of CO_2 molecules adsorbed in the heterogeneous pore was less than that in the homogeneous pore, while the specified pore volume was the same. This leads to a lower value of adsorbed amount in the case of a heterogeneous slit pore at high pressures.

(d) The smaller pore with NH_4OH can enhance CO_2 adsorption better than the larger pore not only the effect of NH_4OH but also the effect of confined space.

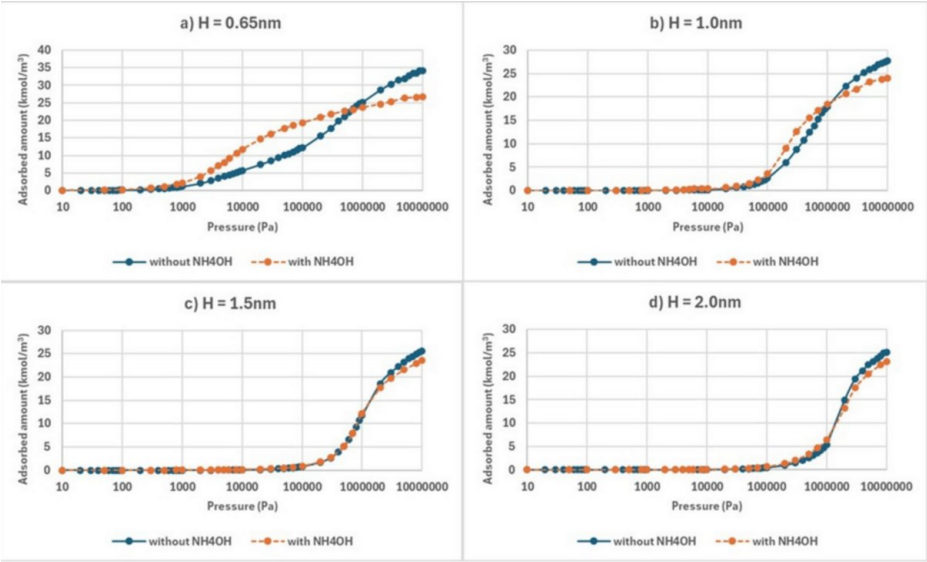

FIGURE 10: Simulation results for CO2 adsorption in carbon slit pores having widths of (a) 0.65, (b) 1.0, (c) 1.5, and (d) 2.0 nm at 273K in the presence and absence of NH4OH

Comparison between experimental data and combined isotherm

The GCMC simulation results obtained for finite-length carbon slit pore varied from 0.65 to 5.0 nm, together with the experimental data for CO_2 adsorption in activated carbon containing 0.5% NH_4OH, were used to determine the pore size distribution (PSD) by using the optimization solver of the Excel program. Figure *11* shows a comparison between the combined adsorption isotherm (symbol with line) and experimental data (symbol) for CO_2 adsorption at 298K. The combined isotherm agreed quite well with the experimental result, with the regression coefficient (R^2) greater than 0.95. Figure *12* presents the pore size distribution obtained for activated carbon with 0.5% NH_4OH. The result showed a bimodal distribution, with most micropores in the range of less than 1.0 nm and the mesopores between 1.5 and 3.0 nm. The total pore volume obtained from the optimization method using the GCMC was 0.0801 cc/g, which was quite close to that obtained from experimental data of 0.0909 cc/g. Therefore, the simulation results using GCMC can be used to determine the PSD of the absorbent and to describe the adsorption mechanism of CO_2 into the activated carbon quite well. The micropore of activated carbon appeared to have a significant effect on CO_2 adsorption.

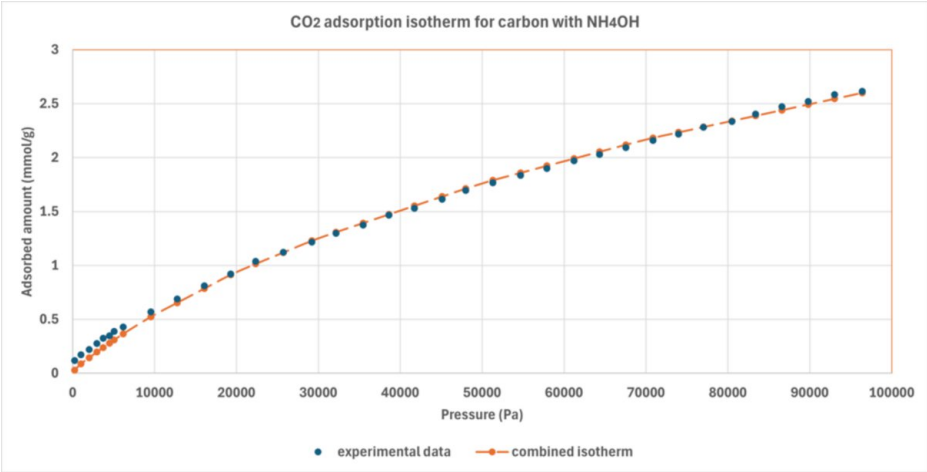

FIGURE 11: Comparison between experimental data (symbol) and combined adsorption isotherms (symbol with line) for CO2 adsorption in activated carbon at 298K

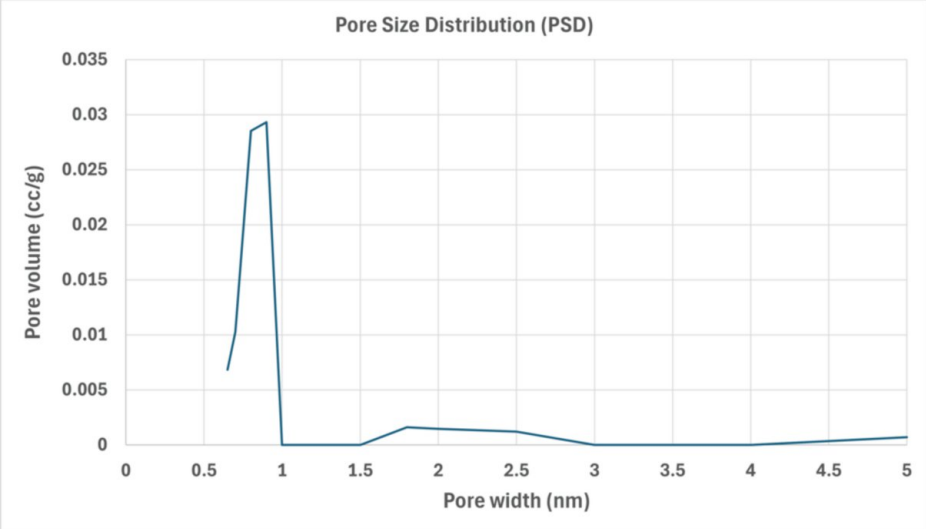

FIGURE 12: Pore size distribution obtained for activated carbon with 0.5% NH4OH using the GCMC simulation

GCMC, Grand Canonical Monte Carlo

Conclusions

This study examined the effects of TEA and NH_4OH impregnation in activated carbon on CO_2 capture performance. The findings demonstrate that TEA and NH_4OH loading significantly influences the pore structure and CO_2 adsorption capacity of the activated carbon. Physical treatment with the CO_2 gasification process resulted in AC-P, a material with a high surface area but limited CO_2 adsorption compared to chemically treated carbons in the case of TEA. Chemical treatment with TEA solutions introduced amine groups onto the activated carbon surface, enhancing the CO_2 adsorption capacity. However, excessively high TEA loading (above 5%) led to pore blocking, hindering CO_2 diffusion and reducing adsorption capacity. The optimal TEA concentration for achieving maximum CO_2 adsorption capacity was found to be 1 wt%. At this concentration, TEA creates favorable surface chemistry for CO_2 capture without significantly compromising the pore structure. In the case of NH_4OH, the pore volume increases with an increase of NH_4OH loading, and the adsorption of CO_2 in carbon with NH_4OH was greater than that without NH_4OH. These findings suggest that TEA and NH_4OH impregnation can be a viable strategy for improving the CO_2 capture performance of activated carbon. However, careful optimization of the TEA and NH_4OH loading is crucial to balance the creation of favorable adsorption sites with the maintenance of a well-developed pore structure for efficient CO_2 diffusion. This work is particularly valuable for its simple preparation method and low-cost pre-treatment of commercial activated carbon, making it suitable for industrial applications.

Additional Information

Author Contributions

All authors have reviewed the final version to be published and agreed to be accountable for all aspects of the work.

Concept and design: Atichat Wongkoblap, Suravit Naksusuk, Tanyarat Khongkhuntian

Acquisition, analysis, or interpretation of data: Atichat Wongkoblap, Suravit Naksusuk

Drafting of the manuscript: Atichat Wongkoblap, Suravit Naksusuk

Critical review of the manuscript for important intellectual content: Atichat Wongkoblap, Suravit Naksusuk, Tanyarat Khongkhuntian

Supervision: Atichat Wongkoblap, Suravit Naksusuk

Disclosures

Human subjects: All authors have confirmed that this study did not involve human participants or tissue. **Animal subjects:** All authors have confirmed that this study did not involve animal subjects or tissue. **Conflicts of interest:** In compliance with the ICMJE uniform disclosure form, all authors declare the following: **Payment/services info:** All authors have declared that no financial support was received from any organization for the submitted work. **Financial relationships:** All authors have declared that they have no financial relationships at present or within the previous three years with any organizations that might have an interest in the submitted work. **Other relationships:** All authors have declared that there are no other relationships or activities that could appear to have influenced the submitted work.

Acknowledgements

Funding to Suravit Naksusuk is supported from Institute of Engineering, Suranaree University of Technology.

References

1. Russell L: 5.11 - Carbonaceous particles: source-based characterization of their formation, composition, and structures. Treatise on Geochemistry (Second Edition). Holland D (ed): Oxford, Elsevier, 2014. 291-316. 10.1016/B978-0-08-095975-7.00415-0
2. Nanda S, Dalai AK, Berruti F, Kozinski JA: Biochar as an exceptional bioresource for energy, agronomy, carbon sequestration, activated carbon and specialty materials. Waste and Biomass Valorization. 2016, 7:201-35. 10.1007/s12649-015-9459-z
3. Metz B, Davidson O, Coninck HD, Loos M, Meyer L: The IPCC Special Report on Carbon dioxide Capture and Storage. 2005.
4. Mukherjee A, Okolie JA, Abdelrasoul A, Niu C, Dalai AK: Review of post-combustion carbon dioxide capture technologies using activated carbon. Journal of Environmental Sciences. 2019, 83:46-63. 10.1016/j.jes.2019.03.014
5. Li B, Duan Y, Luebke D, Morreale B: Advances in CO2 capture technology: A patent review. Applied Energy. 2013, 102:1439-447. 10.1016/j.apenergy.2012.09.009
6. Aaron D, Tsouris C: Separation of CO2 from flue gas: A review. Separation Science and Technology. 2005, 40:321-48.
7. Florides GA, Christodoulides P: Global warming and carbon dioxide through sciences. Environment International. 2009, 35:390-401. 10.1016/j.envint.2008.07.00
8. Leung DYC, Caramanna G, Maroto-Valer MM: An overview of current status of carbon dioxide capture and storage technologies. Renewable and Sustainable Energy Reviews. 2014, 39:426-43. 10.1016/j.rser.2014.07.093
9. Zecca A, Chiari L: Fossil-fuel constraints on global warming. Energy Policy. 2010, 38:1-3. 10.1016/j.enpol.2009.06.068
10. Aghel B, Janati S, Wongwises S, Shadloo MS: Review on CO2 capture by blended amine solutions. International Journal of Greenhouse Gas Control. 2022, 119:103715. 10.1016/j.ijggc.2022.103715
11. Mohd Azmi NZ, Buthiyappan A, Abdul Raman AA, Abdul Patah MF, Sufian S: Recent advances in biomass based activated carbon for carbon dioxide capture - A review. Journal of Industrial and Engineering Chemistry. 2022, 116:1-20. 10.1016/j.jiec.2022.08.021
12. Chen S, Yue Q, Gao B, Li Q, Xu X, Fu K: Adsorption of hexavalent chromium from aqueous solution by modified corn stalk: A fixed-bed column study. Bioresource Technology. 2012, 113:114-20. 10.1016/j.biortech.2011.11.110
13. Chen J, Yang J, Hu G, et al.: Enhanced CO2 capture capacity of nitrogen-doped biomass-derived porous carbons. ACS Sustainable Chemistry & Engineering. 2016, 4:1439-445. 10.1021/acssuschemeng.5b01425
14. Naksusuk S, Tangsathitkulchai C: Carbon dioxide capture in a fixed bed of coconut shell activated carbon impregnated with sodium hydroxide: effects of carbon pore texture and alkali loading. Engineering Journal. 2019, 23:29-48. 10.4186/ej.2019.23.4.29
15. Phothong K, Tangsathitkulchai C, Lawtae P: The analysis of pore development and formation of surface functional groups in bamboo-based activated carbon during CO2 activation. Molecules. 2021, 26:5641. 10.3390/molecules26185641
16. Corti HA, Fiaschi D, Lombardi L: Carbon dioxide removal in power generation using membrane technology. Energy. 2004, 29:2025-43. 10.1016/j.energy.2004.03.011
17. Hidayu AR, Muda N: Preparation and characterization of impregnated activated carbon from palm kernel shell and coconut shell for CO2 capture. Procedia Engineering. 2016, 148:106-13. 10.1016/j.proeng.2016.06.463
18. Khalil SH, Aroua MK, Daud WMAW: Study on the improvement of the capacity of amine-impregnated commercial activated carbon beds for CO2 adsorbing. Chemical Engineering Journal. 2012, 183:15-20. 10.1016/j.cej.2011.12.011
19. Lee CS, Ong YL, Aroua MK, Daud WMAW: Impregnation of palm shell-based activated carbon with sterically hindered amines for CO2 adsorption. Chemical Engineering Journal. 2013, 219:558-64. 10.1016/j.cej.2012.10.064
20. Saxena R, Singh VK, Kumar EA: Carbon dioxide capture and sequestration by adsorption on activated carbon. Energy Procedia. 2014, 54:320-29. 10.1016/j.egypro.2014.07.275
21. Tan YL, Islam MA, Asif M, Hameed BH: Adsorption of carbon dioxide by sodium hydroxide-modified granular coconut shell activated carbon in a fixed bed. Energy. 2014, 77:926-31. 10.1016/j.energy.2014.09.079
22. Mohammad NK, Ghaemi A, Tahvildari K: Hydroxide modified activated alumina as an adsorbent for CO2 adsorption: Experimental and modeling. International Journal of Greenhouse Gas Control. 2019, 88:24-37. 10.1016/j.ijggc.2019.05.029
23. Tangsathitkulchai C, Naksusuk S, Wongkoblap A, Phadungbut P, Borisut P: Equilibrium and kinetics of CO2 adsorption by coconut shell activated carbon impregnated with sodium hydroxide. Processes. 2021, 9:201.

10.3390/pr9020201
24. Brunauer S, Emmett H, Teller E: Adsorption of gases in multimolecular layers. Journal of the American Chemical Society. 1938, 60:309-19. 10.1021/ja01269a023
25. Lippens BC, de Boer JH: Studies on pore systems in catalysts: V. The t method. Journal of Catalysis. 1965, 4:319-23. 10.1016/0021-9517(65)90307-6
26. Ngernyen Y, Tangsathitkulchai C, Tangsathitkulchai M: Porous properties of activated carbon produced from Eucalyptus and Wattle wood by carbon dioxide activation. Korean Journal of Chemical Engineering. 2006, 23:1046-54. 10.1007/s11814-006-0028-9
27. Ravikovitch PI, Vishnyakov A, Russo R, Neimark AV: Unified approach to pore size characterization of microporous carbonaceous materials from N-2, Ar, and CO2 adsorption isotherms. Langmuir. 2000, 16:2311-320. 10.1021/la991011c
28. Frenkel D, Smit B: Understanding Molecular Simulation (second edition). Academic Press, New York; 2002.
29. Wongkoblap A, Junpirom S, Do DD: Adsorption of Lennard-Jones fluids in carbon slit pores of a finite length. A computer simulation study. Adsorption Science & Technology. 2005, 23:1-18. 10.1260/0263617053737163
30. Lawtae P, Phothong K, Tangsathitkulchai C, Wongkoblap A: Analysis of gas adsorption and pore development of microporous-mesoporous activated carbon based on GCMC simulation and a surface defect model. J. Porous Materials. 2024, 31:51-67. 10.1007/s10934-023-01493-5
31. Borisut P, Tangsathitkulchai C, Wongkoblap A, Nuchitprasittichai A, Phothong K: Carbon dioxide capture in NaOH impregnated activated carbon: simulation and experimental studies. Adsorption. 2025, 31:82. 10.1007/s10450-025-00633-4
32. Fortes AD, Brodholt JP, Wood IG, Vočadlo L, Jenkins HDB: Ab initio simulation of ammonia monohydrate (NH3·H2O) and ammonium hydroxide (NH4OH). The Journal of Chemical Physics. 2001, 115:7006-14. 10.1063/1.1398104
33. Harris JG, Yung KH: Carbon dioxide's liquid-vapor coexistence curve and critical properties as predicted by a simple molecular model. The Journal of Physical Chemistry. 1995, 99:12021-2024. 10.1021/j100031a034
34. Johnson JK, Zollweg JA, Gubbins KE: The Lennard-Jones equation of state revisited. Molecular Physics. 1993, 78:591-618. 10.1080/00268979300100411
35. Ozaki Y: Near-Infrared spectroscopy—its versatility in analytical chemistry. Analytical Sciences. 2012, 28:545-63. 10.2116/analsci.28.545